This is a pre-print version of: Nuti, A., Bertini, F., Cipolla, V. et al. Design of a Fuselage-Mounted Main Landing Gear of a Medium-Size Civil Transport Aircraft. Aerotec. Missili Spaz. 97, 85–95 (2018). https://doi.org/10.1007/BF03405803

Design of a Fuselage-Mounted Main Landing Gear of a Medium-Size Civil Transport Aircraft

A. Nuti[a], F. Bertini[a], V. Cipolla[a], G. Di Rito[a]

[a] University of Pisa
Department of Civil and Industrial Engineering - Aerospace Division

Abstract

The subject of the present paper is the design of an innovative fuselage mounted main landing gear, developed for a PrandtlPlane architecture civil transport aircraft with a capacity of about 300 passengers. The paper presents the conceptual design and a preliminary sizing of landing gear structural components and actuation systems, in order to get an estimation of weight and of the required stowage. The adopted design methodology makes use of dynamic modelling and multibody simulation from the very first design stages, with the aim of providing efficient and flexible tools for a preliminary evaluation of performances, as well as enabling to easily update and adapt the design to further modifications. To develop the activity, the multibody dynamics of the landing gear (modelled using Simpack software) has been integrated via co-simulation with dynamic models developed in the Matlab/Simulink environment.

1. Introduction

The case study analyzed in the paper is an innovative PrandtlPlane civil transport aircraft, based on an intuition of L. Prandtl, who postulated the box wing as the lifting system with minimum induced drag. Aerodynamic features have been firstly investigated in [1], and a number of studies followed in recent years [3]. The reference aircraft, in particular, is the subject of the European project PARSIFAL (Prandtlplane ARchitecture for the Sustainable Improvement of Future AirpLanes). The conceptual design stage has led to the definition of a baseline aircraft configuration (Fig. 1 and Tab. 1). The lifting system is a box wing with the positively swept front wing positioned on the lower fuselage and the rear wing on top of two fins. Thus, the main landing gear must be centrally positioned on the bottom fuselage.

Many solutions of fuselage-mounted landing gear exist both for civil and military transport aircraft with high wing configurations.
In military aircraft, landing gear is often stowed in external pods in order to maximize cargo capacity, and the gear is designed to operate on rough unpaved runways (solutions are deeply dependent on this requirement).
In civil aircraft, some examples exist for small-medium sized vehicles, and the main landing gear is usually stowed inside a fuselage bay.

In the present case, a solution is designed taking into account constraints imposed by the aircraft architecture; the main driving concepts are dynamic performance, to limit impact loads and enhance comfort, and minimum frontal section, for reducing aerodynamic drag. The influence of landing gear pods shape is considered in detail in the aircraft aerodynamic design.

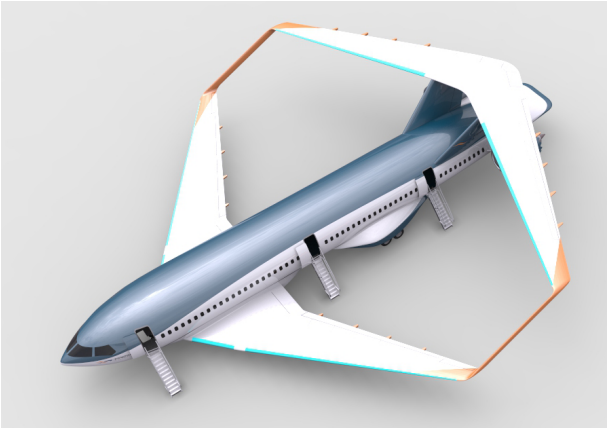

Figure 1. PARSIFAL aircraft.

2. Landing gear requirements

The primary functions of the landing gear system, from which general requirements arise, are listed in [4], [5], [6]. The unconventional architecture of Parsifal leads to the definition of additional constraints:

Table 1
Aircraft data.

Overall length (m)	44
Wing span (m)	36
Maximum Take-Off Weight (kg)	121000
Maximum Landing Weight (kg)	95000
Seats, single class	310

Ground clearance The ground clearance of the fuselage is set 800 mm in order to facilitate loading and unloading operations with on-board airstairs.

Stowage The main landing gear must be located into lateral pods outside the fuselage cross section, Fig. 2, in order to avoid the interruption of the cargo deck and provide enough cargo capacity for LD3-45 containers.

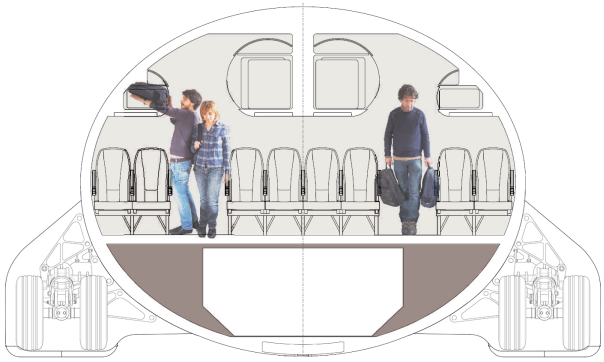

Figure 2. Fuselage cross section and gear stowage.

Actuation Conventional gears use hydraulic actuation for the required functions (retraction/extension, door actuation, locking/unlocking in up or down positions, wheel braking, steering). Within Parsifal project, "more electric" types of actuation are considered; as a matter of fact, in the next decades the only primary power available on board could be the electric one, following the great effort done to move towards the "all electric" aircraft [9] [10] [11].

3. General layout

3.1. Geometrical constraints

Landing gear location is determined for the reference configuration according to [6], [7].

Fig. 3 shows the principal parameters regarding landing gear longitudinal position; recommended limits for the nose gear static load are $6 \div 20\%$ of aircraft weight.

Concerning the lateral requirements, the horizontally enlarged fuselage cross section of Parsifal leads to a satisfactory wheel track, related to turnover angle. The other constraint is wing tip clearance, since there are no wing-mounted engines.

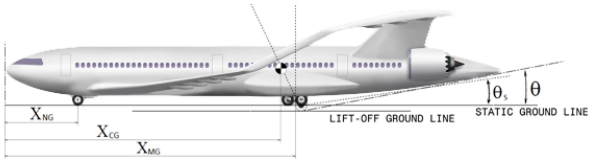

Figure 3. Longitudinal requirements on gear location.

3.2. Wheels

The number and layout of wheels is primarily determined from flotation considerations, i.e. the runway ability to support the aircraft weight; the main parameters influencing flotation are the load per tyre, tyre diameter, tyre inflation pressure, but also airfield surface characteristics.

The required number of wheels can be readily obtained from an overview of existing commercial aircraft; in the present case four wheels per main gear are adopted, having a dual tandem configuration, with two wheels per axle due to safety considerations in case of a flat tyre.

Flotation performance can be then assessed using *Aircraft Classification Number* (ACN) method, developed by ICAO and expressing the relative effect of an aircraft on the runway pavement. The selected wheel layout results in better flotation performance than A320 and B737-800, even though Parsifal MTOW is about 50% higher.

Airworthiness regulations [8] prescribe load rating requirements for aircraft tyres (CS 25.733). Suitable tyres for main and nose gear are reported in Tab. 2; modern radial tubeless tyres are chosen.

4. Main landing gear design

Some significant fuselage-mounted conceptual solutions have been examined, e.g. C-130, C-27J, C-141, A400M. A discussion of the advantages and drawbacks of the different solutions can be found in [12].

Among the concepts examined, the final choice is a single telescopic suspension and bogie; the resulting main gear is shown in Fig. 4 (refer to [12] for a detailed description).

Each gear is equipped with an oleo-pneumatic shock strut and carries a bogie with two axles and four wheels. A structural framework supports the landing

Table 2
Tyre data.

	Main LG	Nose LG
Number of tyres	8 (4 × 2)	2
Tyre model	H40×14.5 R19	36×11 R16
	[dia.×width−rim dia. (in)]	
Max. static load (kg)	14605	9525
Ply rating	24	20
Inflation pressure, unloaded (bar)	13.8	12.8

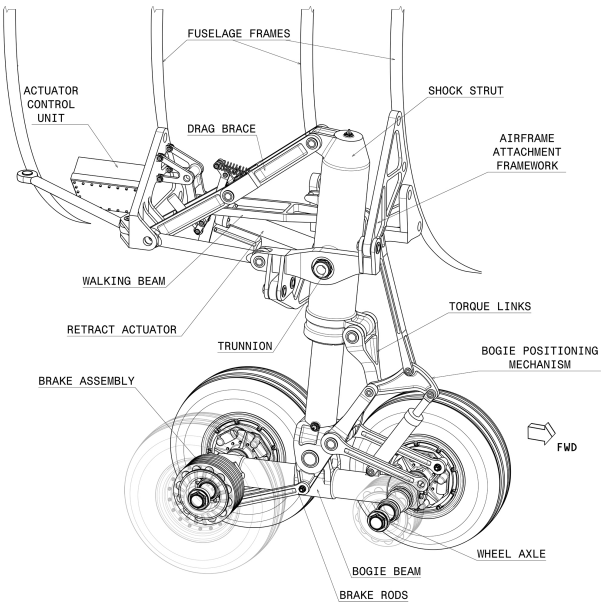

Figure 4. Main landing gear.

gear assembly and is connected to two main frames, transferring ground loads to the fuselage. The gear retracts forward in pods at the sides of the fuselage (Fig. 2) in such a way to minimize the frontal area during flight.

4.1. Shock absorber

A two-stage oleo-pneumatic shock strut is used in the proposed design [7]. The high pressure chamber is in the inner cylinder and it is delimited by a floating piston, while the outer cylinder forms the low pressure chamber, in which the gas is mixed with oil. This configuration allows a large stroke with limited overall length. To achieve high efficiency the orifice cross-section is varied over the stroke by means of a metering pin; some other orifices are made different for compression and recoil, in order to limit the rebound. The shock strut is connected to the airframe structure by a trunnion and it is held in down position by the drag brace, Fig. 4.

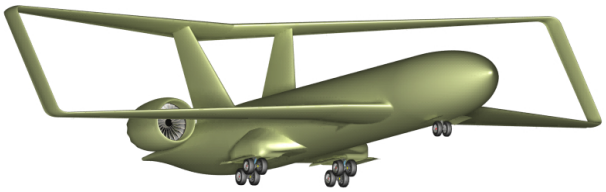

Figure 5. Aircraft with landing gear extended.

Table 3
Shock absorber sizing results.

First stage initial pressure (bar)	55
Second stage initial pressure (bar)	110
Maximum stroke (mm)	550
Static stroke @MTOW (% max. stroke)	85%
Static gas pressure @MTOW (bar)	170
Maximum (endstroke) gas pressure (bar)	220

The driving condition for shock absorber sizing is the landing impact. The approximate vertical wheel stroke required can be estimated according to [7], by considering the work done by vertical forces during touchdown and applying the work-energy theorem.
The present design features a maximum stroke of 550 mm; the resulting reaction factor N, such that NW is the maximum ground reaction during touchdown, is $N = 0.9$ at the limit sink speed $V_{sink} = 3.05\,\mathrm{m/s}$ (10 ft/s).

The relevant shock absorber design parameters are reported in Tab. 3; gas pressures are chosen according to guidelines from literature [7], however static values are slightly increased in order to limit shock strut weight and section width. Sizing of the orifices cross sections and metering pin is done considering results from drop test simulations (section 6.7).

4.2. Brakes

A preliminary brake sizing is made in a system perspective, in order to estimate weights and sizes to be used in the landing gear design.
The method is based on simple models and statistical data, starting from requirements [8] considering only the *design landing stop* condition (CS 25.735).

Carbon-carbon composite multidisk brakes are considered in the proposed design, as standard equipment for modern aircraft; typical material characteristics are shown in Tab. 4.

Table 4
Brake disk material characteristics [7] [13].

Density (kg/m^3)	1700
Sp. thermal capacity @300°C (J/kg/K)	1400
Max. pressure at friction surface (MPa)	1.5
Max. long duration temperature (°C)	$700 - 1000$
Coeff. of friction of one disk on another	$0.35 - 0.45$

Each brake absorbs an amount of energy equal to

$$E = \frac{\gamma W V^2}{2 g N_w}$$

where N_w is the number of braked wheels, V is the initial speed ($V = V_{ref}/1.3$ for the *design landing stop*) and γ is the fraction of the initial aircraft kinetic energy converted into brake internal energy.

A required heat pack mass of 35 kg is obtained assuming $\gamma = 0.9$ (in a conservative manner) and considering a temperature increment of 500 °C (standard operation). A 9-disk arrangement is chosen, and brake housing and actuation are added to the brake assembly (Fig. 7); the total weight is estimated according to similar existing solutions.

In aircraft landing gears involving multi-axle bogies, the brake stator assemblies (carrying the stator disks and the brake actuation system) are mounted freely on the axles and the braking torque is reacted against rods connecting to the shock strut, called *brake equalizing rods*. This prevents bogie pitching during braking, equalizing brake effectiveness on all the wheels.

4.3. Extension/retraction system

The gear retracts forward and up into the fuselage pod; retraction kinematics are designed to correctly position the wheels when extended, while minimizing stowage when retracted. An actuator causes the shock strut to rotate about the trunnion, while a *bogie positioning mechanism* ensures correct positioning of the wheels during retraction/extension (Fig. 6).

A folding drag brace stabilizes the shock strut in the longitudinal direction while it is in down position. An irreversible mechanism located between the two segments of the drag brace automatically locks the gear in down position. An uplock mechanism is also present, consisting of a hook assembly on the airframe attachment, engaging a roller located on the aft side of the shock strut. Additional actuating systems provide for the locks release.

Regulations require an emergency "free-fall" mode which assures gear extension by gravity in case of a complete loss of power on board. For this reason, the uplock include a manual release device in case of failure of the primary system. In the present case, retracting the gear forward is an advantage as aerodynamic drag helps in case of a free-fall extension.

4.3.1. Bogie positioning

Landing gear multi-axle bogies are usually set at a certain incidence in down position, so that one wheelset touches down before the other, extending the total compression stroke of the gear (useful for raising the tail clearance) and improving shock absorption capacity. A damper is connected to the bogie beam in order to limit its pitching oscillations, while the correct position for retraction is mantained by a spring or adjusted by a more complex actuation system.

The designed bogie positioning mechanism is shown in Fig. 6, and consists of a triangular bellcrank, bogie pitch damper, and a positioning link which runs down to a fixed point in the airframe structure. This particular mechanism allows to position the bogie beam so that it is horizontal in the retracted position and at an angle of 70 degrees with shock strut in the down standby position. The tilting action is supplied directly by the rotation of the shock strut about the trunnion.

The damper allows bogie pitching during touchdown, while its preload returns the bogie in the correct position for retraction after liftoff.

It can be noted that the large bogie tilting angle during retraction requires specific positioning of hinges and brake rods in order to avoid interference while achieving the right kinematic operation and brake rods effectiveness.

4.3.2. Actuation

Electrically powered (*power-by-wire*) actuators, in particular Electro-Mechanical Actuators (EMA), are chosen. EMAs are already used in brakes, and several research programs have focused on electromechanical steering and retract actuators [14] [15]. However, difficulties are still present, for example in providing a damped free-fall backup mode in case of actuator screw jamming. Reliability issues are a primary concern for EMAs in aircraft applications [16]; health monitoring and fault isolation are necessary for safe operation [17] [18].

At the present stage only a preliminary sizing of the actuator is performed, reserving study of fail-safe devices to future work.
Retraction and extension of the gear is provided by a linear EMA, as it offers the possibility of easily achieving a high reduction ratio and allows the use of a smaller and lighter electric motor.

The actuator is mounted in a closed kinematic structure, Fig. 8: the retract actuator and the so-called *walking beam* are both pinned to the shock strut at

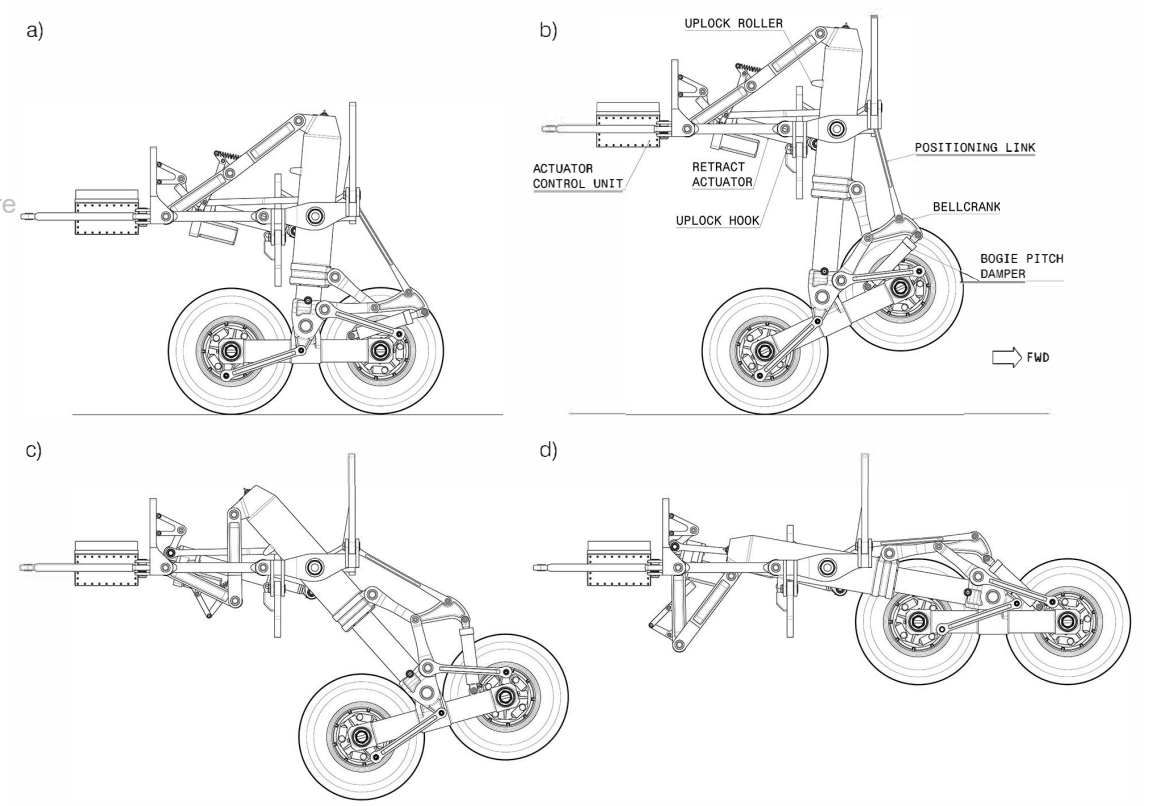

Figure 6. MLG retraction kinematics and bogie positioning mechanism.

one end and to the same bolt at the other, forming a closed system of forces in which retraction load goes back to the trunnion. A third element, here called *hanger*, acts as a pendulum and transfers to the airframe only the component of the resultant force on the common pin parallel to the hanger itself. This solution has the advantage of minimizing the reaction force applied to the airframe, and also reduces the required actuation force.

The considered requirements on gear extension/retraction actuation are the following:

- vertical load factor up to 1.5;
- airspeed up to 113 m/s (220 knots);
- maximum time of 10 s to complete retraction.

Retraction loads are calculated with reference to a simplified schematics (Fig. 10), where loading is quasi-static and forces deriving from door actuation are disregarded. Aerodynamic forces are considered by taking into account only a drag component parallel to the fuselage axis, and the variation of drag during retraction is approximated with a parabolic function of the retraction angle, Fig. 9. Maximum drag F_{max} is estimated considering results from literature [19] and statistical data on gear drag.

Fig. 11 shows forces acting on actuator, walking beam and aeroplane structure; the actuator force in case of direct actuation (without walking beam) is also included, highlighting the beneficial effect of the mechanism on actuator and airframe loads.

The designed actuator is composed of a DC permanent-magnet brushless motor and a planetary roller screw; parallel-axis configuration is chosen, with a spur gear reducer linking the motor shaft with the screw. Actuator preliminary sizing considers two basic requirements, stall load and no-load speed; results are given in Tab. 5.

5. Structural sizing

Finite Element linear stress analyses of the main landing gear components and the airframe attachment structure are conducted in order to perform a preliminary sizing and get an estimation of the structural weight, under ultimate load cases derived from airworthiness regulations [8], section *Ground Loads*; dynamic loads are obtained from simulations of landing gear operation in these conditions.

A first evaluation of fatigue life is also performed using safe-life design methodology. This approach is based on: estimation of load spectrum, elastic stress

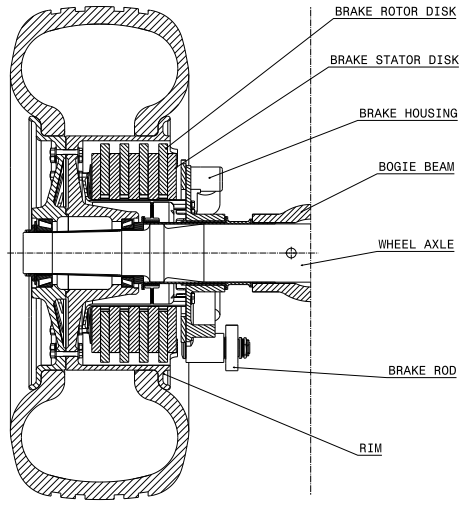

Figure 7. Wheel section.

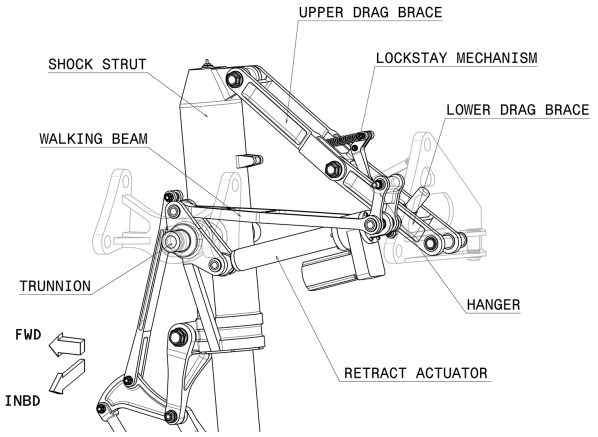

Figure 8. Retraction mechanism.

analysis, use of S-N curves, use of a cumulative damage rule (Miner). The target life of main landing gear components is set to 75000 flight cycles. Then a safety factor of 5 is chosen for taking scatter in material properties and in load spectrum into account. In order to get a preliminary estimation of the load history during standard operations, a reference landing condition is considered, with a sink speed equal to 0.9 m/s (3 ft/s), and 1.8 m/s^2 (6 ft/s^2) constant deceleration braking; minor load cycles are disregarded.

Traditional materials for landing gears are high-strength steels; however, according to recent tendencies, titanium alloy Ti6Al4V is used in this work for all main structural parts.

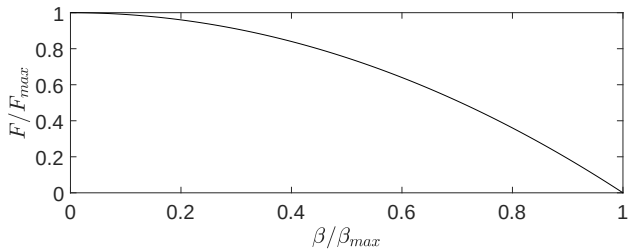

Figure 9. Variation of aerodynamic load with retraction angle β ($\beta = 0 \rightarrow$ gear extended).

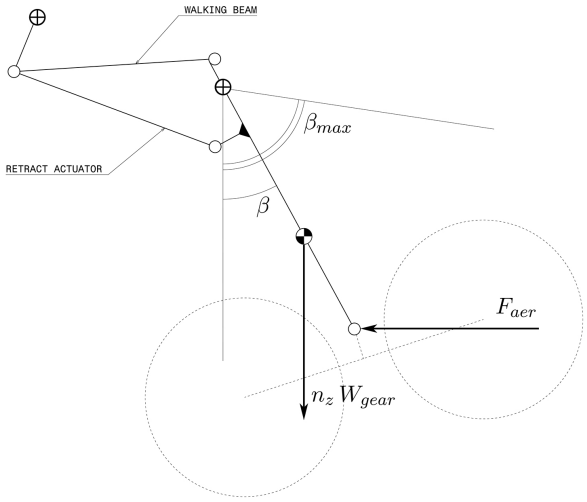

Figure 10. Main gear retraction loads schematic.

5.1. Landing gear weight estimation

Considering results of the preliminary sizing, the main landing gear weight breakdown is reported in Tab. 6. The total mass of the resulting landing gear system, composed of nose and main gears, including the airframe attachment structure, is equal to 4270 kg, corresponding to 3.5% of MTOW, which accords with statistical data [6] [7].

6. Modelling and simulation

6.1. Co-simulation technique

The assessment of dynamic loads acting on the landing gear and on the surrounding structure is a fundamental aspect of the design process of both the gear and the airframe; this task is conveniently performed using multibody simulation (MBS), a well-estabilished method for studying aircraft ground dynamics. An introduction to multibody dynamics can be found in [20]. Many MBS softwares are available and allow to

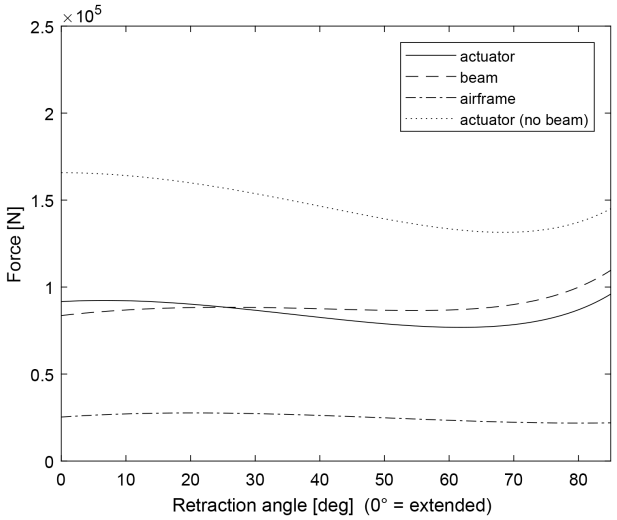

Figure 11. Main gear retraction loads.

Table 5
Main landing gear retraction actuator data.

Max. force (kN)	100
Total stroke (mm)	470
Max. speed (mm/s)	70
Screw diameter×lead (mm)	39×5
Screw efficiency	0.75
Gear ratio	3.0
Gearbox efficiency	0.97
Max. motor torque (N m)	36
Max. motor speed (rpm)	2500
Max. motor power (kW)	9.6
Linear unit weight (kg)	46
Motor+gearbox weight (kg)	25
Electronics weight (kg)	18
Total weight (kg)	89

easily set up complex dynamic models; simulation can be conveniently used from the very first stages of the design, when it enables to evaluate dynamic behaviour, to analyse more configurations, and to correct problems as early as possible, which is especially useful in case of a new concept of aircraft.

The present analyses are carried out by means of Simpack multibody code and Matlab/Simulink software, used in co-simulation[1]. This approach offers the advantages of multibody simulation and also easily integrates models developed in Matlab/Simulink environment, which allows more flexible dynamic modelling and control design.

[1]The two models run simultaneously and exchange information at a fixed sample rate, called *communication interval*; each one solves its own set of equations, including as inputs the data received from the other at the previous step.

Table 6
Main landing gear weight breakdown.

Component	Mass (kg)
Tyre	58 (×4)
Rim	36 (×4)
Brake	75 (×4)
Brake rods	6 (×4)
Bogie beam & Axles	210
Shock absorber	475
Positioning mechanism	70
Retract actuator	89
Retraction mechanism	75
Airframe attachment	280
Total weight	1900

A fixed-step Runge-Kutta method is chosen in Simulink, with a step size of 10^{-4} s, equal to the communication interval. Variable-step solver SODASRT2 is used in Simpack.

6.2. Multibody models

Once landing gear kinematics has been defined, Simpack multibody models are set up to simulate the relevant load cases; set up and verification of the models is done gradually starting from very simple cases.

An introduction to Simpack and its modelling elements is given in [21]. A feature called *Substructure* allows to reuse a model inserting it one or more times into a bigger model; for drop tests a *Body* representing the test mass is connected to the main gear *Substructure*, while for landing simulations both main and nose gears are connected to a *Body* representing the airframe.

The main gear is modelled with rigid bodies connected by ideal joints. The shock strut outer cylinder is supported by a rigid joint: once the forces and moments acting on it are known, the transmission of loads to the trunnion and drag brace is statically determined and it is calculated in the post-processing phase; furthermore, brake rods kinematics is not modelled as the main focus is studying the landing impact. The main gear model topology diagram is shown in Fig. 12.

Sensor elements are added to measure the following quantities, then transmitted to Simulink via the co-simulation interface:,

- velocity of the aircraft CG expressed in body axes;
- aircraft angular rates expressed in body axes;
- shock absorber strokes and their time derivatives.

The inputs received from Simulink are:

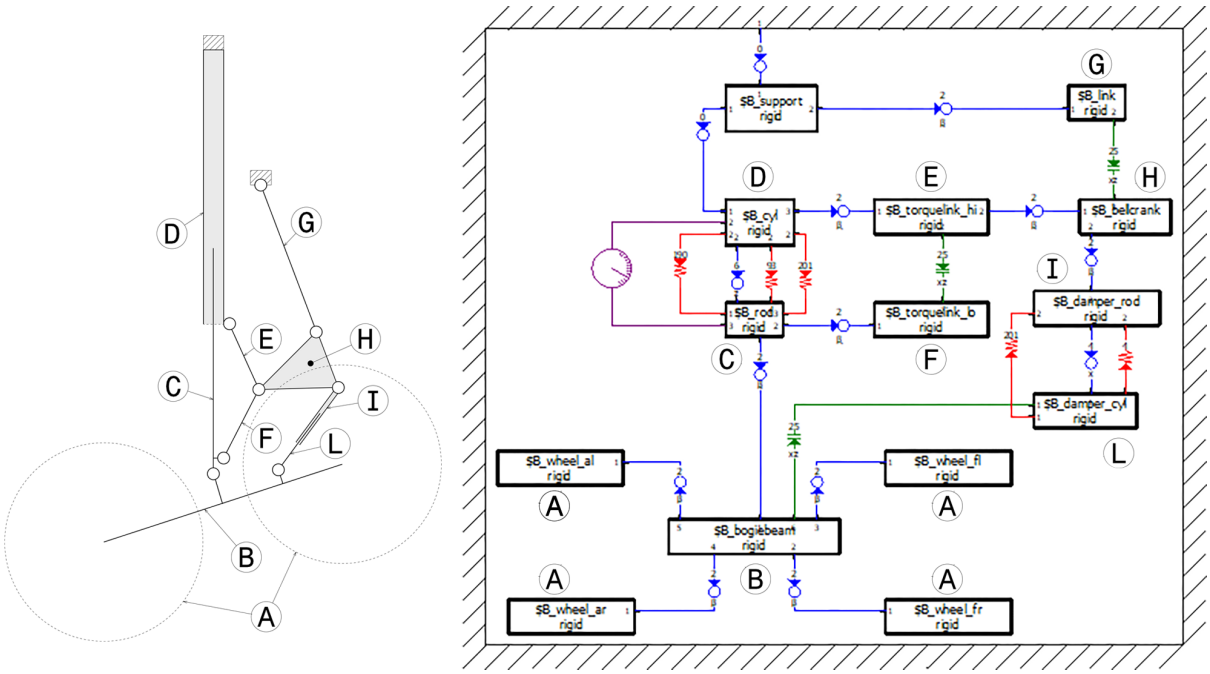

Figure 12. Main landing gear multibody model diagram.

- aerodynamic forces and moments acting on the aircraft CG, expressed in body axes;
- forces acting on shock struts;

these inputs are introduced into the multibody model by *Force/Torque by u(t)* elements.

Other used Force Elements are:

- *Spring-damper parallel*, used in the bogie pitch damper;
- *Bump Stop*, i.e. a high stiffness unilateral spring-damper, used for endstroke representation;
- *Stick-slip*, used for modelling the shock strut seal friction;
- *MF-Tyre*, used for modelling tyre-runway interaction.

6.3. Tyre-runway interaction

Tyre forces and moments are introduced into the multibody model by *MF-Tyre* force elements, acting between each wheel and a specific *Road* element representing the runway surface. The force element requires a *Tire parameter file* containing the relevant physical and empirical coefficients; it implements Pacejka's Magic Formula tyre model [22] for steady-state contact forces and moments, and is capable of simulating also tyre transient behaviour [23]. In the present case, steady-state Magic Formula is used, and only longitudinal tyre behaviour is considered, since simulations are restricted to symmetrical manoeuvres. A reduced set of vertical and longitudinal parameters is defined, with typical values for aircraft tyres of similar size.

6.4. Shock absorber model

The main landing gear oleo-pneumatic shock absorber is described in section 4.1; a section view and the relative schematic diagram are shown in Fig. 13.

A simplified analytical model of the shock absorber is developed and implemented in Simulink; this allows rapid assessment of the influence of the design parameters (gas pressures, orifice areas) on dynamic performance. The following assumptions are made:

- incompressible oil;
- polytropic transformation of the gas $PV^n = P_0V_0^n$, with $n = 1.3$;
- friction of seals neglected in this model.

With these hypotheses, we can determine the gas volume and pressure in the two chambers as a function of the stroke (x) only: $P_L(x)$, $P_H(x)$. Hydraulic flows Q_I, Q_E depend on $\dot{x}$ and determine the pressure drop across the orifices

$$\Delta P = \frac{1}{2}\rho_h k_s (Q/A_s)^2 \mathrm{sgn}(Q)$$

given the oil density ρ_h, orifice cross section A_s and pressure drop coefficient k_s.

From equilibrium considerations we can calculate the total force acting on the strut:

$$F_{strut} = P_L(A_L - A_I) + (P_H + \Delta P_I)A_I - (P_L + \Delta P_E)A_E.$$

The system of equations is implemented in Simulink, resulting in a simulation block that calculates the force

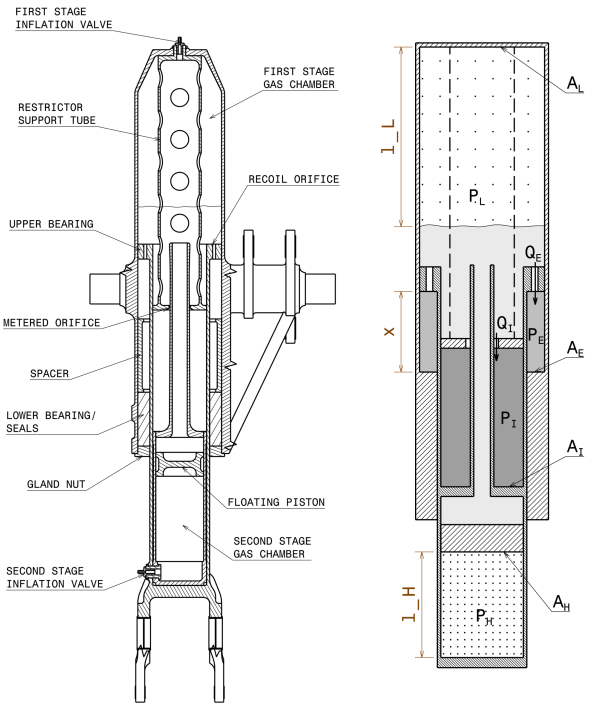

Figure 13. Shock strut section and schematic diagram.

applied to the strut as a function of the stroke x and its time derivative $\dot{x}$.

6.5. Aerodynamic forces

When simulating the landing impact of the full aeroplane it is necessary to consider the actual aerodynamic forces acting on the airframe. In particular, lift should be approximately equal to aircraft weight upon landing and might be heavily decreased by the activation of ground spoilers after touchdown. These effects are complex and difficult to describe in detail in a preliminary design phase, when accurate low-speed aerodynamic data are not yet available.

A linearised model is used for the description of aerodynamic forces; additional terms are added to the force perturbations in order to obtain a simple representation of lift dumping effect caused by ground spoiler deployment. Approximate values of the stability derivatives are obtained from preliminary aerodynamic analyses of the aircraft in landing configuration. The model is implemented as a Matlab function and included via Simulink co-simulation.

6.6. Test cases

The following limit load cases are defined by regulations [8], CS 25.473:

- MTOW, sink speed 1.83 m/s (6 ft/s);
- MLW, sink speed 3.05 m/s (10 ft/s).

6.6.1. Drop test conditions

Drop tests are simulated under the limit load cases; in addition, a reserve energy condition (MLW, sink speed 3.7 m/s) is considered, under which the shock absorber must not fail (CS 25.723).

The effect of lift is considered by using an equivalent reduced test mass, such as the test mass W_e moving by distance d (tyre deflection plus shock absorber stroke) does the same work of the entire aircraft weight W but with lift L doing opposite work during that displacement

$$W_e h + W_e d = Wh + W(1 - L/W)d.$$

This imposes that the shock absorber in the test must dissipate approximately an equal amount of energy than in the real case. The free drop height $h = V_{sink}^2/2g$ is determined in order to obtain the desired sink speed; a value of $L/W = 1$ is assumed.

6.6.2. Landing conditions

Regulations require to consider a number of attitudes and speeds for landing loads evaluation. However, for the sake of simplicity, the analysis in the case of a reference symmetric landing manoeuvre is presented.

The aircraft is initially trimmed; the flight path angle is set to obtain the specified sink speed. No pilot commands are applied to counteract the pitching acceleration generated by ground reaction forces when the aircraft contacts the runway with the main gears. For each landing case a simulation is performed with and without activation of ground spoilers. Landings in the limit conditions are simulated; also, a “normal” condition (MLW, sink speed 0.9 m/s) is considered.

6.7. Simulation results

Dynamic loads acting on gear components are obtained from simulations, as they can be read as joint forces in Simpack.

Data from drop test simulations are used for landing gear structural verification, since they represent the limit impact loads. Fig. 14 shows an example of shock absorber vertical load vs. stroke curve, obtained from the drop test; we can note that steady-state load is lower than the real static one because of the reduced test mass.

Drop tests with both still and rotating wheels have been simulated, and sensitivity studies have been performed by varying the bogie pitch damping, shock strut seal friction and orifice areas. Dynamic simulation turned out to be a powerful design tool, in this case especially useful for shock absorber dynamic tuning, and for sizing the bogie positioning mechanism. Fig. 15 shows that damping of the bogie pitch damper heavily influences the loads applied to the mechanism. The damping value is therefore adjusted to improve dynamic behaviour, while limiting forces, in order to reduce weight of the connected components.

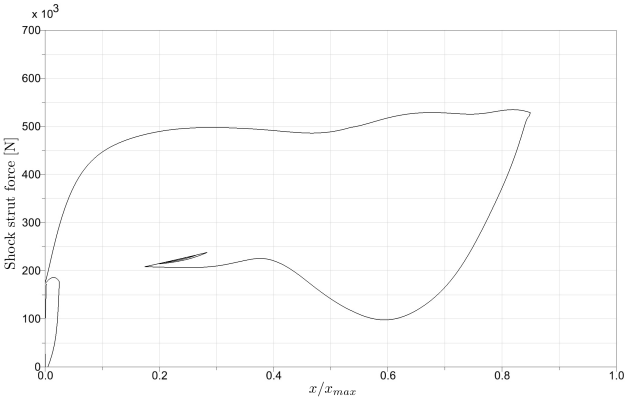

Figure 14. Shock absorber load-stroke curve (Drop test, MLW, sink speed 3.05 m/s).

An example of landing simulation results is shown in Fig. 16. It may be noted that lift dumping have a pronounced effect on the final equilibrium stroke and load on wheels, while it has small influence on peak impact loads, because the effect becomes substantial after the first compression of the shock strut.

The maximum vertical ground reaction is reached in static conditions except for extremely hard landings. In fact, ground reaction factor N is often less than one during impact, according to preliminary energy considerations (section 4.1), while it is $N = 1$ in static conditions. However, landing impact might be a critical condition for the airframe, and structural dynamics must be investigated.

It is worth noting that landing loads are generally about 10% lower than those obtained in the relative drop test case, showing that in this case the representation of lift by means of an equivalent reduced mass leads to a conservative drop test condition.

Spin-up force in the landing simulation is similar to the spinning wheels drop test, and the peak value is within 25% of the vertical load, which is the limit value considered by regulations.

Conclusions

The present work has led to the definition of a fuselage-mounted main landing gear configuration, satisfying specific requirements imposed by the unconventional aircraft layout of PARSIFAL project.

The obtained landing gear can be adapted to future modifications of the aircraft, and to possible changes in requirements, such as ground clearance and longitudinal gear location.

The use of a co-simulation approach, integrating a multibody software with Matlab/Simulink, has been

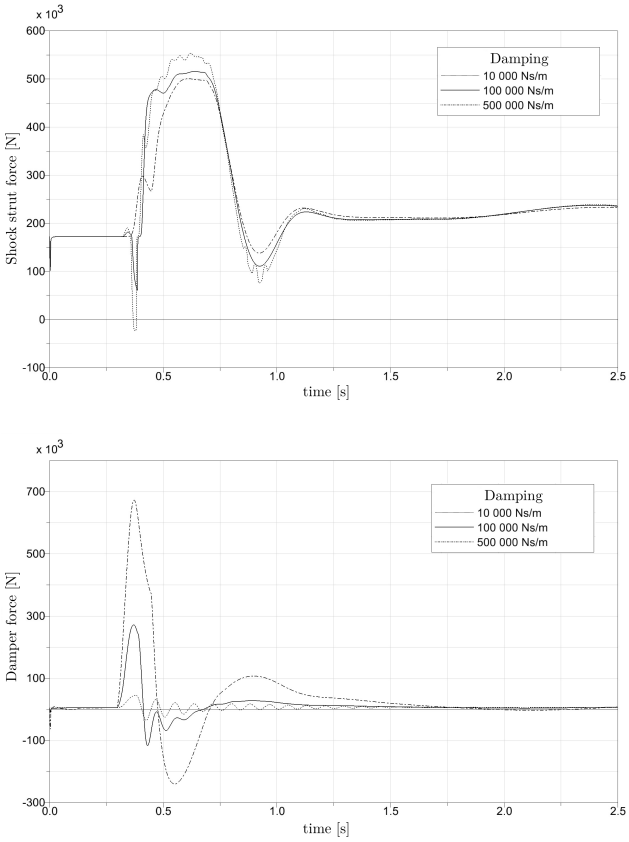

Figure 15. Effect of bogie pitch damping (Drop test, MLW, sink speed 3.05 m/s).

shown to be a reliable and effective tool for preliminary landing gear design; complexity of the models has been gradually increased and the effect of key parameters has been investigated.

Simulations of drop tests and landing conditions have been performed; loads obtained have been used as inputs for Finite Element analyses and preliminary structural sizing. Resulting landing gear system weight is in accordance with statistical data.

Simulation models can be further refined and adapted to future developments of the aircraft design; the effects of flexibility of both airframe and landing gear components could be investigated, as well as more realistic landing manoeuvres; a dynamic braking model could be added.

Multibody simulation models of the entire aircraft could be used to study flight mechanics during takeoff and landing, and to investigate the influence of landing gear design parameters on overall aircraft performance.

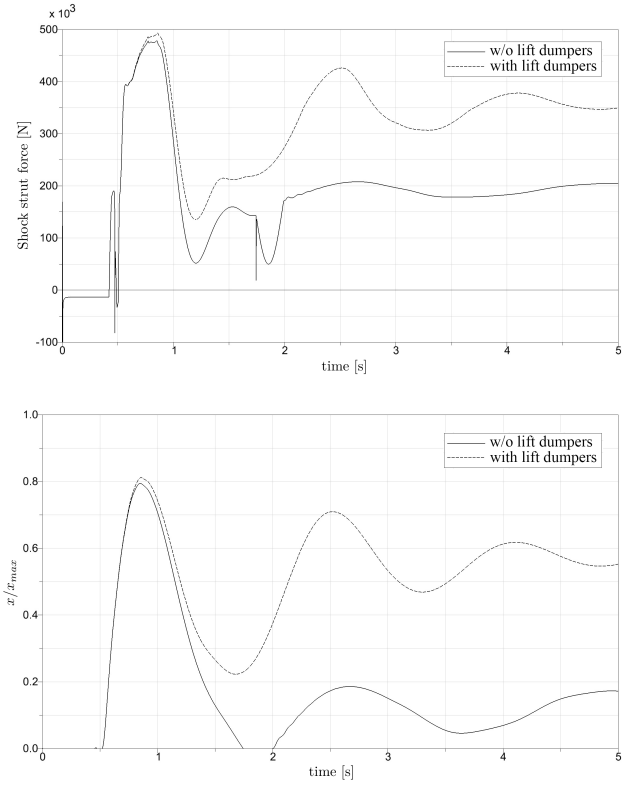

Figure 16. Landing, MLW, sink speed 3.05 m/s.

Acknowledgements

The present paper presents part of the activities carried out within the research project PARSIFAL, which has been funded by the European Union under the Horizon 2020 Research and Innovation Program (Grant Agreement No. 723149).

The authors wish to thank the persons that supported this work with their passion and knowledge; in particular, *46th Air Brigade of the Italian Air Force*, for the support during the initial design stage; *Exemplar Srl* for providing Simpack code; they also wish to thank Dr. Mario Romani, Dr. Guido Saporito and Dr. Michele Grazzini, *Hitachi Rail Italy*, for their valuable suggestions on the set up of multibody models.

REFERENCES

1. A. Frediani, G. Montanari, "Best Wing System: An Exact Solution of the Prandtl's Problem", *Variational Analysis and Aerospace Engineering*, 2009.
2. A. Frediani, V. Cipolla, K. Abu Salem, V. Binante, M. Picchi Scardaoni, "On the Preliminary Design of PrandtlPlane Civil Transport Aircraft", *7th EUCASS conference*, 2017, Milan, Italy.
3. R. Cavallaro, L. Demasi, "Challenges, Ideas, and Innovations of Joined-Wing Configurations: A Concept from the Past, an Opportunity for the Future", *Progress in Aerospace Sciences*, Vol. 87, 2016, pp. 1-93.
4. S.F.N. Jenkins, "Landing Gear Design and Development", *Proceedings of the Institution of Mechanical Engineers*, Vol. 203, No. 1, 1989, pp. 67-73.
5. J. Roskam, " Airplane Design: Part IV - Layout Design of Landing Gear and Systems", 1986.
6. D.P. Raymer, "Aircraft Design: A Conceptual Approach", 1989.
7. N.S. Currey, "Aircraft Landing Gear Design: Principles and Practices", 1988.
8. European Aviation Safety Agency, "Certification Specifications and Acceptable Means of Compliance for Large Aeroplanes CS-25".
9. M. Howse, "All electric aircraft", *IEEE Power Engineering Journal*, Vol. 17, No. 4, 2003, pp. 35-37.
10. J.A. Rosero, J.A. Ortega, E. Aldabas, and L. Romeral, "Moving towards a more electric aircraft", *IEEE Aerospace and Electronic Systems Magazine*, Vol. 22, No. 3, 2007, pp. 3-9.
11. J.C. Shaw, S.D.A. Fletcher, P.J. Norman, and S.J. Galloway, "More electric power system concepts for an environmentally responsible aircraft (N+2)", *Proceedings of 47th International, Universities Power Engineering Conference (UPEC)*, 2012, London, United Kingdom, pp. 1-6.
12. F. Bertini and A. Nuti, "Design and Dynamic Modelling of a Fuselage-Mounted Main Landing Gear for a PrandtlPlane Civil Transport Aircraft", *Master Thesis*, University of Pisa, 2018.
13. A.P. Garshin, V.I. Kulik and A.S. Nilov, "Braking friction materials based on fiber-reinforced composites with carbon and ceramic matrices", *Refractories and Industrial Ceramics*, Vol. 49, No. 5, 2008, pp. 391-396.
14. J.C. Maré, "Aerospace Actuators, Signal-by-Wire and Power-by-Wire", Vol. 2, 2017.
15. G. Di Rito, R. Galatolo, and F. Schettini, "Experimental and simulation study of the dynamics of an electromechanical landing gear actuator", *Proceedings of the 30th International Council of the Aeronautical Sciences (ICAS)*, 2016, Daejeon, South Korea.
16. A. Garcia, I. Cusidò, J.A. Rosero, J.A. Ortega, and L. Romeral, "Reliable electro-mechanical actuators in aircraft", *IEEE Aerospace and Electronic Systems Magazine*, 2008, pp. 19-25.
17. E. Balaban, P. Bansal, P. Stoelting, A. Saxena, K.F. Goebel and S. Curran, "A diagnostic approach for electromechanical actuators in aerospace systems", *Proceedings of the 2009 IEEE Aerospace Conference*, 2009, pp. 1-10.
18. G. Di Rito and F. Schettini, "Health monitoring of electromechanical flight actuators via position-tracking predictive models", *Advances in Mechanical Engineering*, Vol. 10, No. 4, 2018, pp. 1-12.
19. L. Venkatakrishnan, N. Karthikeyan and K. Mejia, "Experimental Studies on a Rudimentary Four Wheel Landing Gear", *AIAA Journal*, Vol. 50, No. 11, 2012, pp. 2435-2447.
20. A.A. Shabana, "Dynamics of Multibody Systems", 3rd ed., 2005.
21. W. Schiehlen (ed.), "Multibody Systems Handbook", 1990.
22. E. Bakker, L. Nyborg, and H.B. Pacejka, "Tyre Modelling for Use in Vehicle Dynamics Studies", *SAE Technical Paper*, No. 870421, 1987.
23. H.B. Pacejka, "Tire and Vehicle Dynamics", 3rd ed., 2012.